

# Separation of Stratiform and Convective Rain Types using Data from an S-band Polarimetric Radar: A Case Study Comparing Two Different Methods

M. Thurai<sup>1</sup>, D. B. Wolff<sup>2</sup>, D. A. Marks<sup>2,3</sup>, C. S. Pabla<sup>2,3</sup>, and V. N. Bringi<sup>1</sup>

<sup>1</sup> Colorado State University, Fort Collins, CO 80523, USA

<sup>2</sup> NASA GSFC Wallops Flight Facility, Wallops Island, Virginia, USA

<sup>3</sup> Science Systems and Applications, Inc., Lanham, MD, USA



# Background

- Stratiform and convective rain are associated with different microphysical and dynamical processes and generally produce drop size distributions (DSDs) with different characteristics.
- The frequency of occurrence of stratiform versus convective rain is generally around 4:1, while in terms of rain volume, it is generally around 2:3 depending on land or ocean; or tropical vs extra-tropics.
- These proportions are important for calculating the vertical profile of net latent heating for applications to storm dynamics and, as a constraint, for numerical weather prediction models.

# Background

- In *Thurai et al. (ECAS-2020)*, a DSD-based separation method for stratiform and convective rain was presented and tested:
  - using disdrometer data from Delmarva peninsula, USA, a mid-latitude coastal region
  - 1 and 3 minute DSDs data from 2DVD + MPS
  - and the NASA-NPOL S-band polarimetric radar observations over the disdrometers for 'visual' validation.
  
- In this paper, we apply the DSD-based technique directly to NPOL radar data and compare with another, independent, well-known, texture-based method (*Steiner et al. 1995*) which utilizes the radar reflectivity and its spatial variability.

## References:

- i. *Steiner, M.; Houze, R.A.; Yuter, S.E. Climatological Characterization of Three-Dimensional Storm Structure from Operational Radar and Rain Gauge Data. J. Appl. Meteor. 1995, 34, 1978–2007.*
  
- ii. *Thurai, M.; Bringi, V.; Wolff, D.; Marks, D.; Pabla, C. Testing the Drop-Size Distribution-Based Separation of Stratiform and Convective Rain Using Radar and Disdrometer Data from a Mid-Latitude Coastal Region. Atmosphere 2021, 12, 392. <https://doi.org/10.3390/atmos12030392>*

# Outline

- Estimating DSD parameters from radar data (S-band)
- NPOL observations: Event on 30 April 2020
- Rain Type Classification
- CFADs
- Summary

# Estimating DSD parameters from radar data

Need to estimate the two main DSD parameters,  $N_W$  and  $D_m$

$N_W$ : Normalized intercept parameter

$D_m$ : Mass-weighted mean diameter

Use NPOL radar reflectivity and differential reflectivity ( $Z_h$  and  $Z_{dr}$ )

The estimation of  $D_m$  is a two-step procedure, the first step involving the estimation of an intermediary parameter,  $D_m'$  which depends on two chosen reference moments, say,  $M_i$  and  $M_j$ .

Then  $D_m'$  is given by:

$$D_m' = \left( \frac{M_j}{M_i} \right)^{\frac{1}{(j-i)}}$$

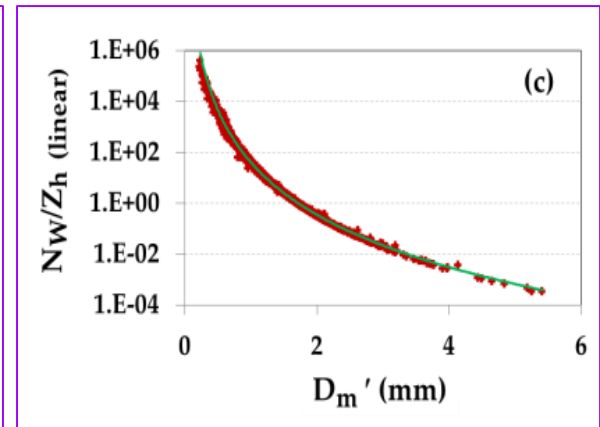
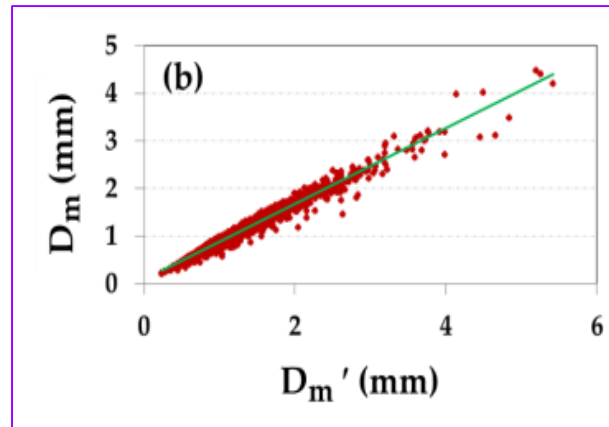
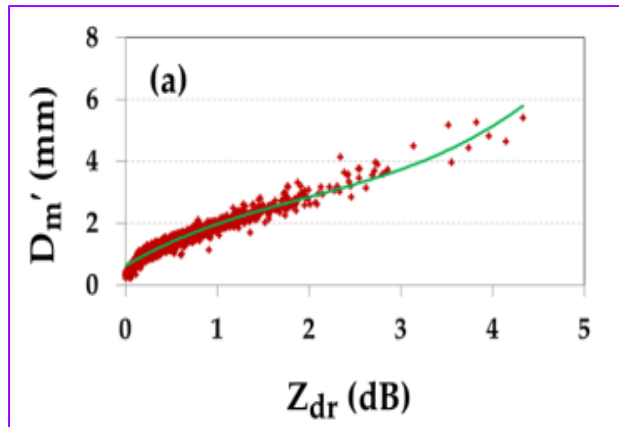
For  $N_W$ , we use

$$N_W = \left( \frac{4^4}{6} \right) N_0' \quad \text{where} \quad N_0' = M_i^{\frac{(j+1)}{(j-i)}} M_j^{\frac{(i+1)}{(i-j)}}$$

# Estimating DSD parameters from radar data

- Estimate  $D'_m$  from  $Z_{dr}$
- Estimate  $D_m$  from  $D'_m$
- Estimate  $N_W$  from  $Z_{h(linear)}$  and  $D'_m$

## S-band scattering simulations using DSD data



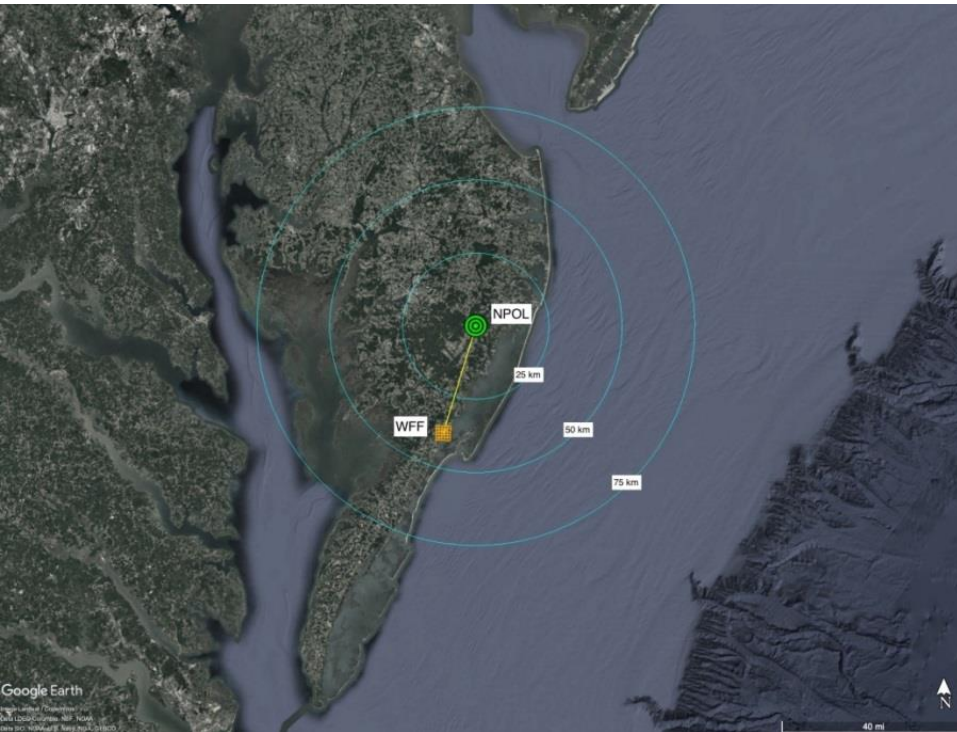
### Fitted curves

(a)  $D'_m = 0.0822 Z_{dr}^3 - 0.4841 Z_{dr}^2 + 1.7515 Z_{dr} + 0.628$

(b)  $D_m = 0.7977 D'_m + 0.0883$

(c)  $\frac{N_W}{Z_{h(linear)}} = 39.446 D'_m^{-6.839}$

# NPOL observations: Event on 30 April 2020



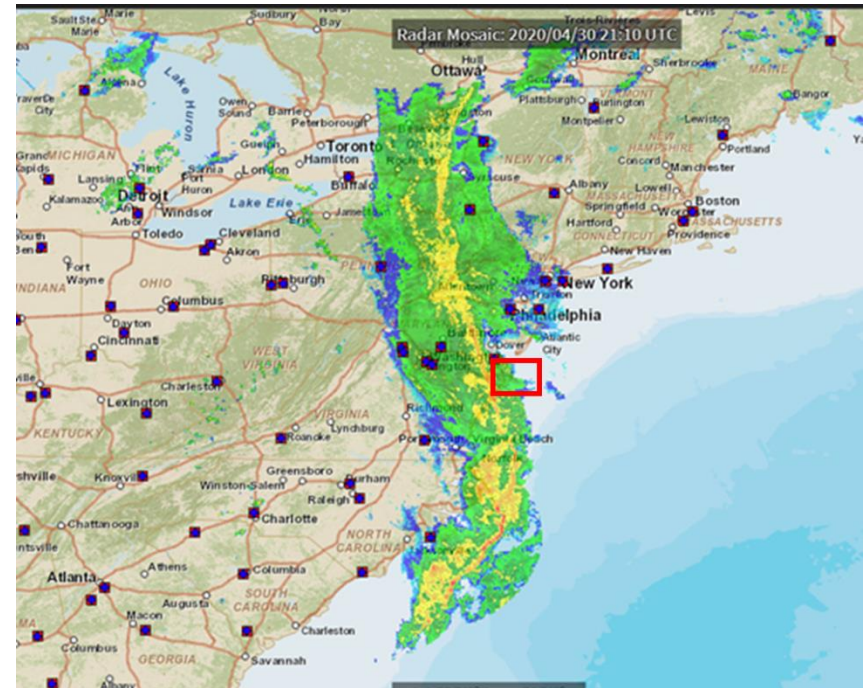
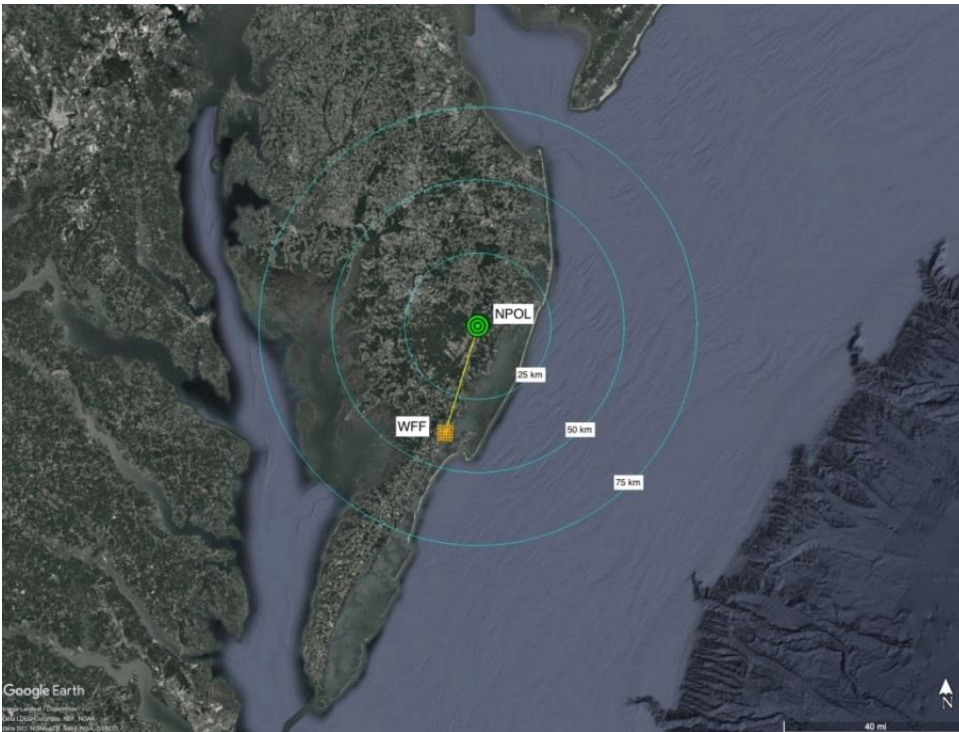
NPOL routine scan sequence includes:

- Volume scans
- RHI scans over the disdrometer site

## 38 km SSW

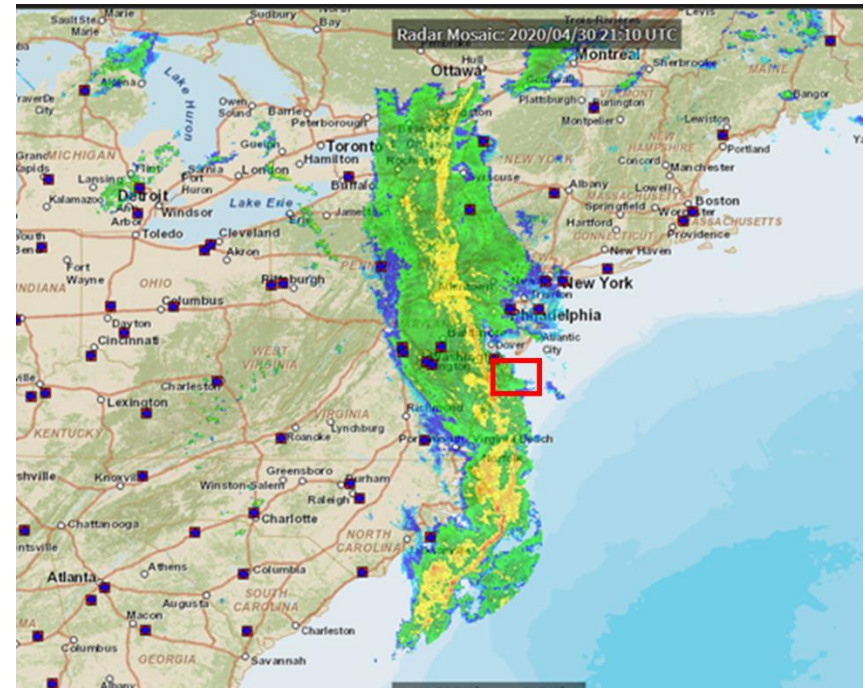
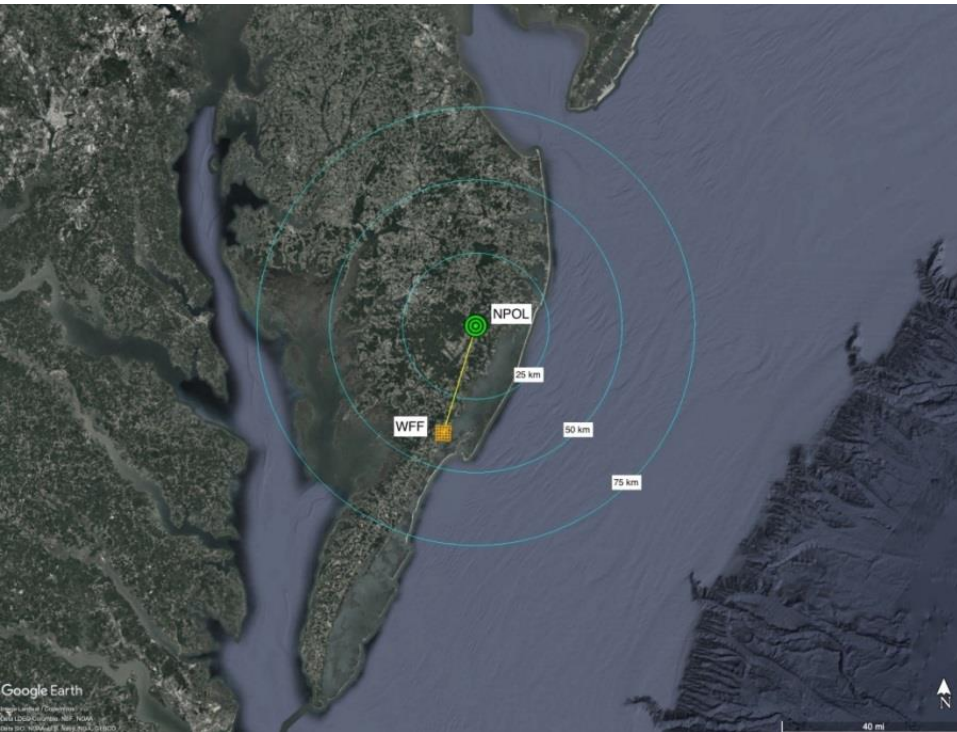
- Network of instruments, including 2DVDs,
- MPS (Meteorological Particle Spectrometer) inside DFIR double wind-fence
- MRR, Pluvio, plus many others

# NPOL observations: Event on 30 April 2020



- On 30 April 2020, a slow moving cold front passed over the WFF region.
- A NW/SE oriented line of strong convection with heavy rain moved through the region.
- Reflectivity within the line was as high as 60 dBZ in areas. The convective line was embedded in stratiform with reflectivity in the range 25 to 35 dBZ.
- As recorded by NASA rain gauges at Wallops, approximately 20 mm accumulated between 19 to 22 h UTC, the majority of which fell within 30 minutes associated with the convective line.

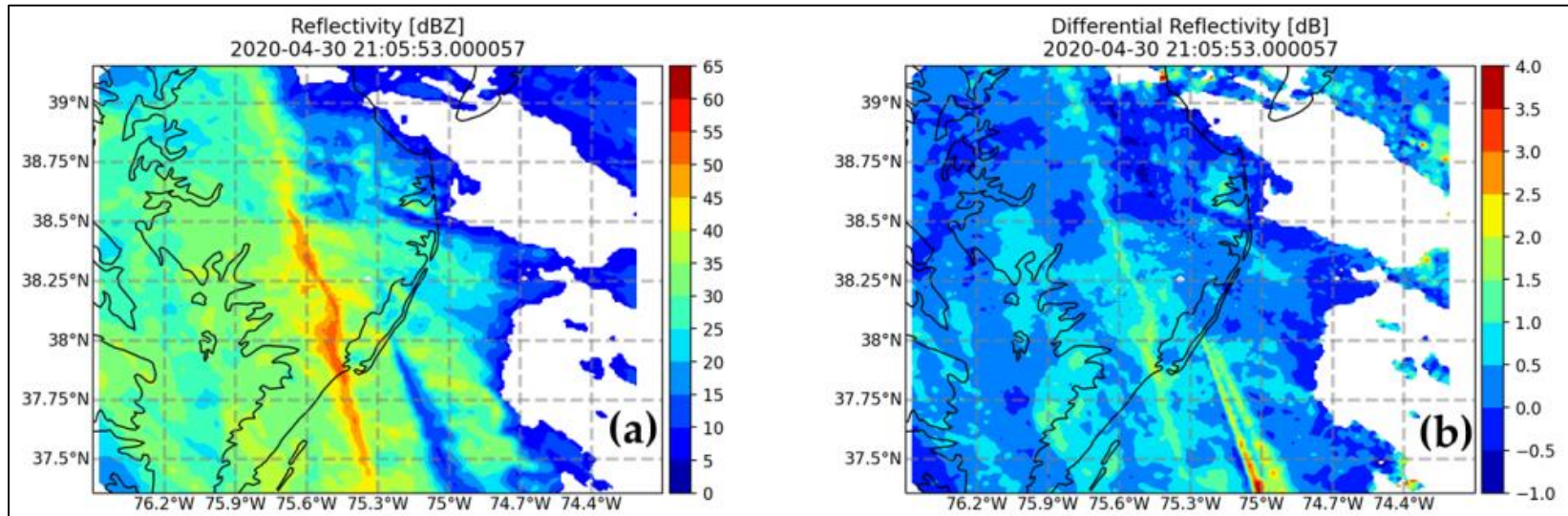
# NPOL observations: Event on 30 April 2020



- From the NPOL volume scans
  - ➔ Gridded data were generated for different altitudes
  - ➔ Lowest at 1000 m a.g.l.
  - ➔ Every 500 m, up to 8000 m a.g.l.

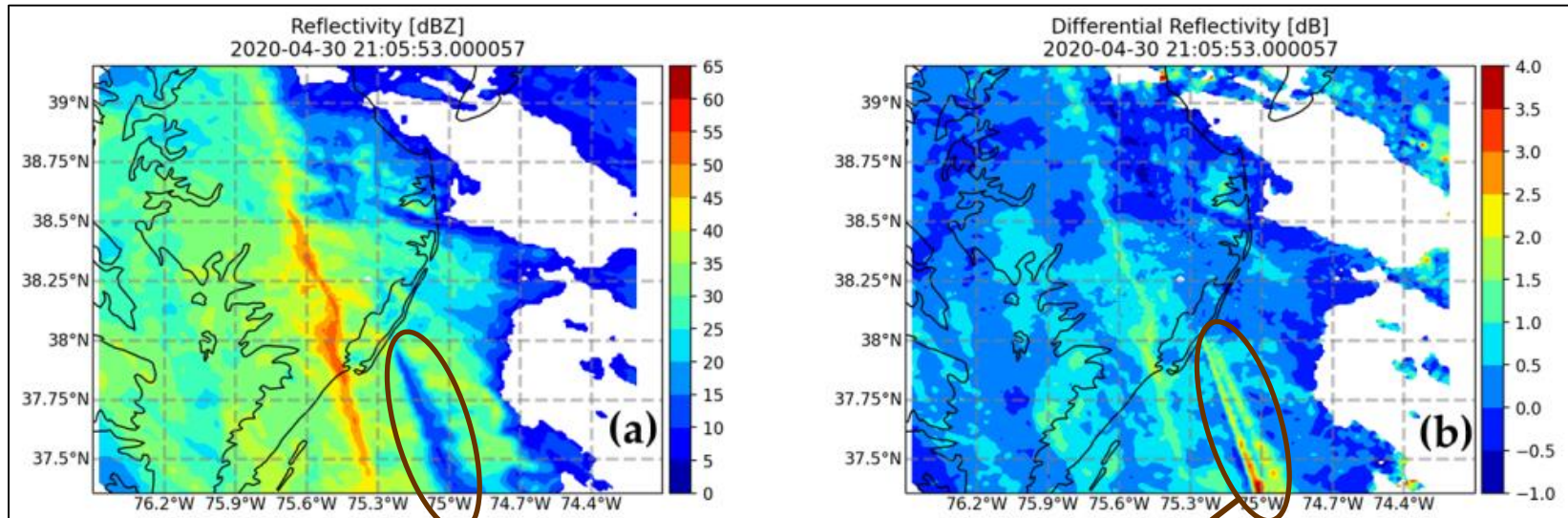
# NPOL observations: Event on 30 April 2020

NPOL gridded data at 1000 m altitude with 500 m by 500 m pixel resolution



# NPOL observations: Event on 30 April 2020

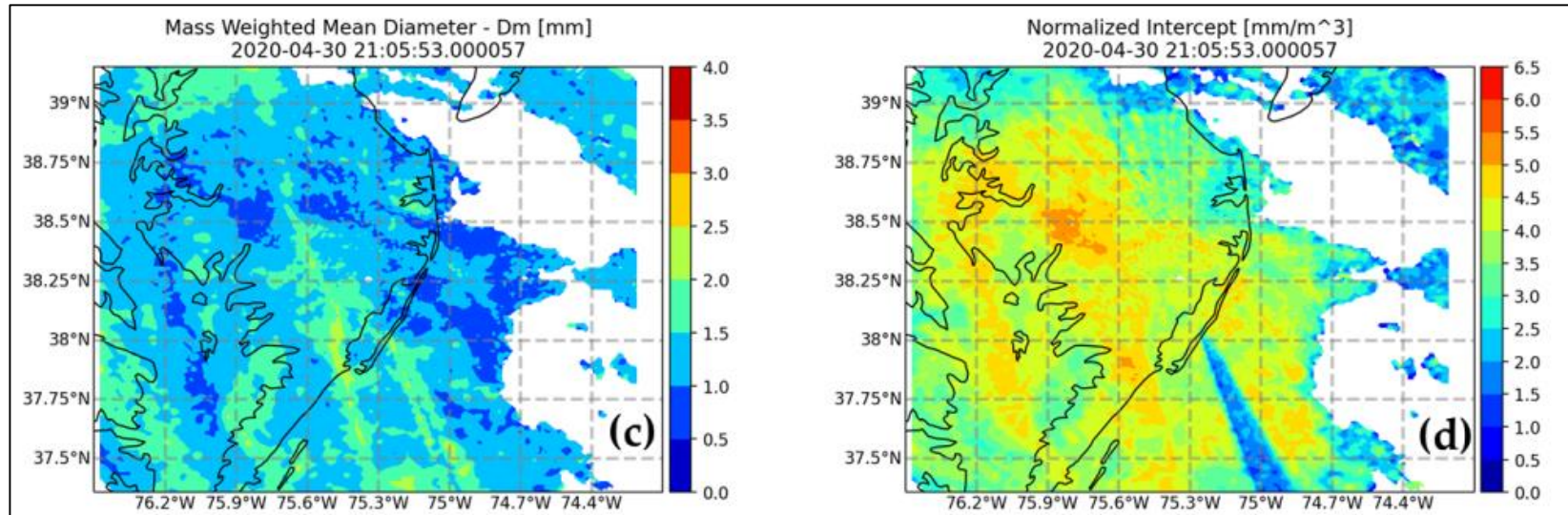
NPOL gridded data at 1000 m altitude with 500 m by 500 m pixel resolution



Beam Blockage  
Hence need to omit  
from analyses

# NPOL observations: Event on 30 April 2020

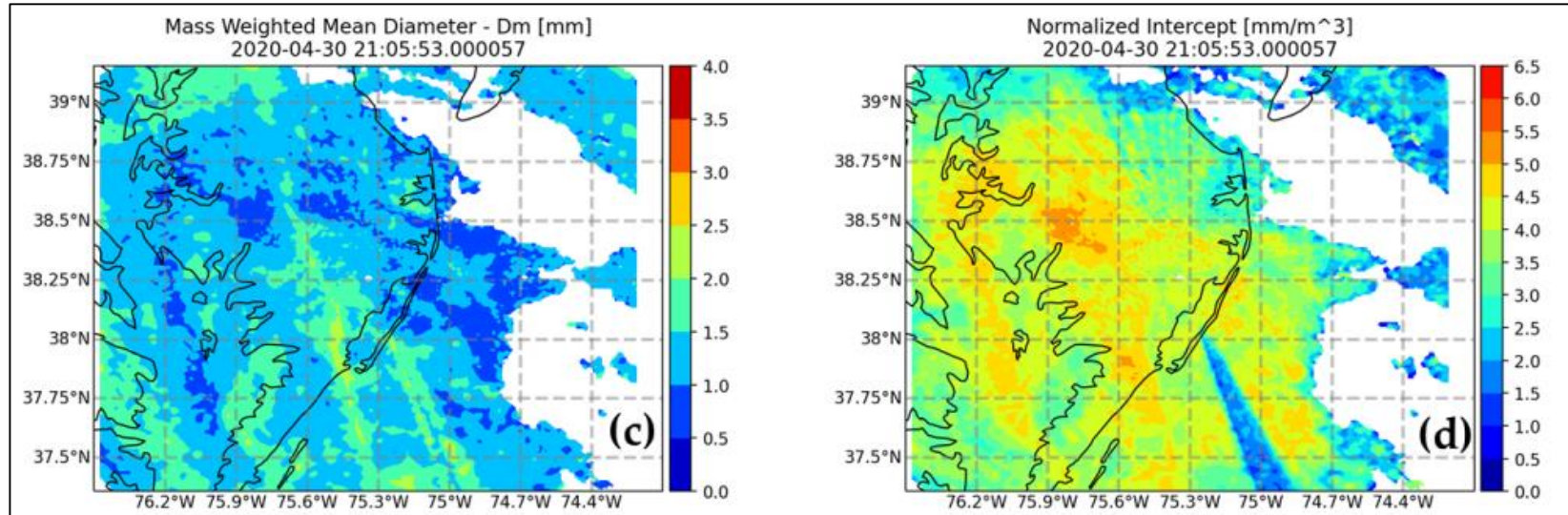
## Estimated $N_W$ and $D_m$ from the gridded data



The gridded data ranging from -60 km to +60 km both in the North-South and the East-West directions were extracted and the classification based on the  $N_W$  -  $D_m$  values for each pixel was determined.

# NPOL observations: Event on 30 April 2020

## Estimated $N_W$ and $D_m$ from the gridded data



A simple 'index' parameter,  $i$  (empirically-derived), was used to indicate whether the  $N_W$  versus  $D_m$  lie above or below the separation line. Value of  $i$  for each pixel is given by:

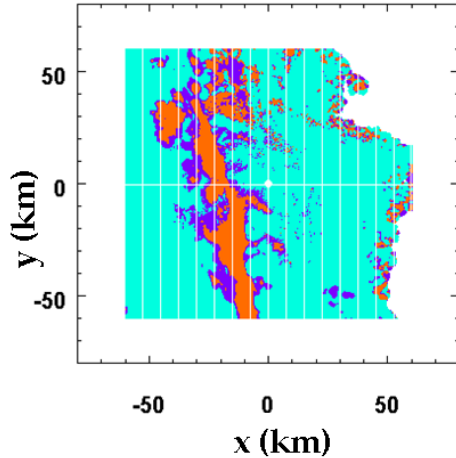
$$i = \log_{10}(N_W^{est}) - \log_{10}(N_W^{sep}) \quad \text{where} \quad \log_{10}(N_W^{sep}) = c_1 D_m^{est} + c_2$$

$N_W^{est}$  is the estimated  $N_W$  for the specific pixel and  $D_m^{est}$  the (corresponding) estimated  $D_m$ . Note: values of  $c_1$  and  $c_2$  may vary somewhat depending on the location, but to be consistent with our previous studies, they were set to  $-1.682$  and  $6.541$ , respectively.

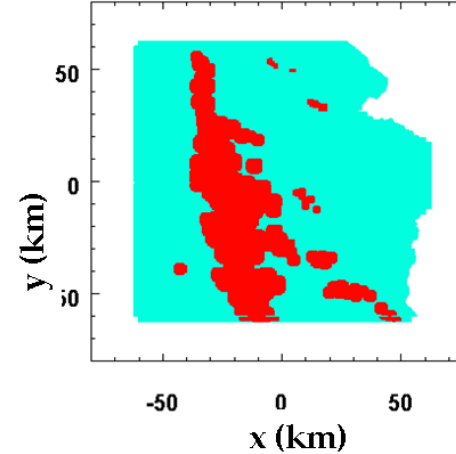
# Rain type classification: Event on 30 April 2020

Stratiform  
Convective  
Mixed

(a) DSD-based classification

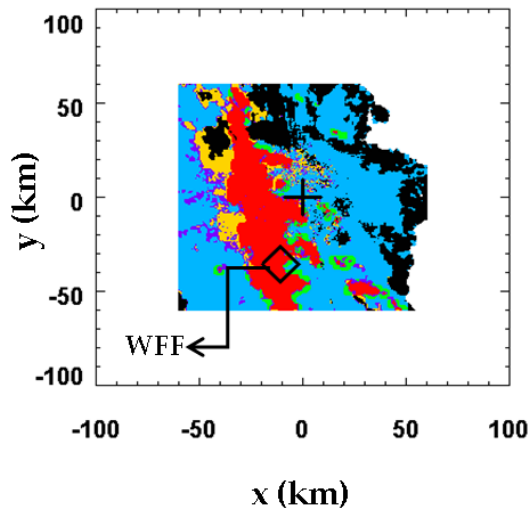


(b) Texture-method



Stratiform  
Convective

(c) Comparison between (a) and (b)



(d) Color code used in (c) and results

Rain type classification by the Texture-based method	Rain type classification by the DSD-based method	Number of radar pixels	Percentage of radar pixels
Stratiform	Stratiform	26313	59%
Convective	Convective	9079	20%
Stratiform	Convective	2914	6%
Convective	Stratiform	2218	5%
N/A	Mixed	4356	10%

# Rain type classification: Event on 30 April 2020

Rain type classification by the Texture-based method	Rain type classification by the DSD-based method	Number of radar pixels	Percentage of radar pixels
Stratiform	Stratiform	26313	59%
Convective	Convective	9079	20%
Stratiform	Convective	2914	6%
Convective	Stratiform	2218	5%
N/A	Mixed	4356	10%

A total of 12% mismatched pixels

- ❖ At S-band, attenuation effects are mostly negligible, but in some regions (beyond the line convection), it did result in  $\sim 0.5$  dB correction for  $Z_h$ .
- ❖ After including these effects, percentage of 'mismatched' pixels reduced from 12% to 11%.

# Contoured Frequency-by-Altitude Diagrams

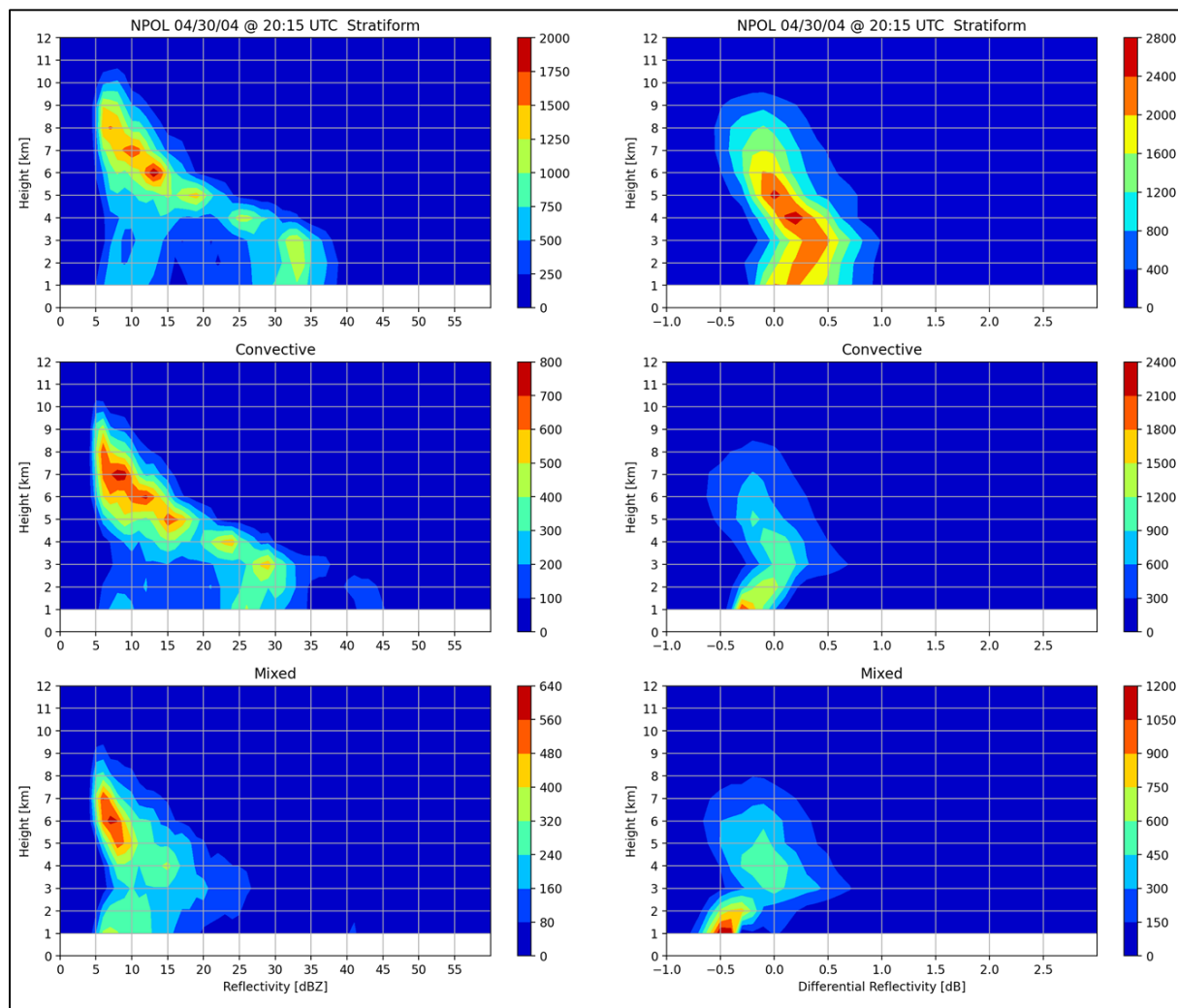
CFADs: useful for examining vertical structures. For the April 30, 2020 case, these were constructed separately for stratiform and convective rain regions (after applying the DSD-based separation), as well as for mixed rain type.

*Left panels* :  $Z_h$  contours

*Right panels* :  $Z_{dr}$  contours

For convective rain (*middle panels*), both  $Z_h$  and  $Z_{dr}$  decrease from 3 down to 1 km, which in turn indicates that drop break-up is the dominant process.

For stratiform rain (*top panels*),  $Z_h$  is almost uniform from 3 to 1 km a.g.l. but  $Z_{dr}$  decreases, indicating, once again, the possible occurrence of drop break process but also indicating an increase in number concentration (per unit volume).



# Contoured Frequency-by-Altitude Diagrams

CFADs:

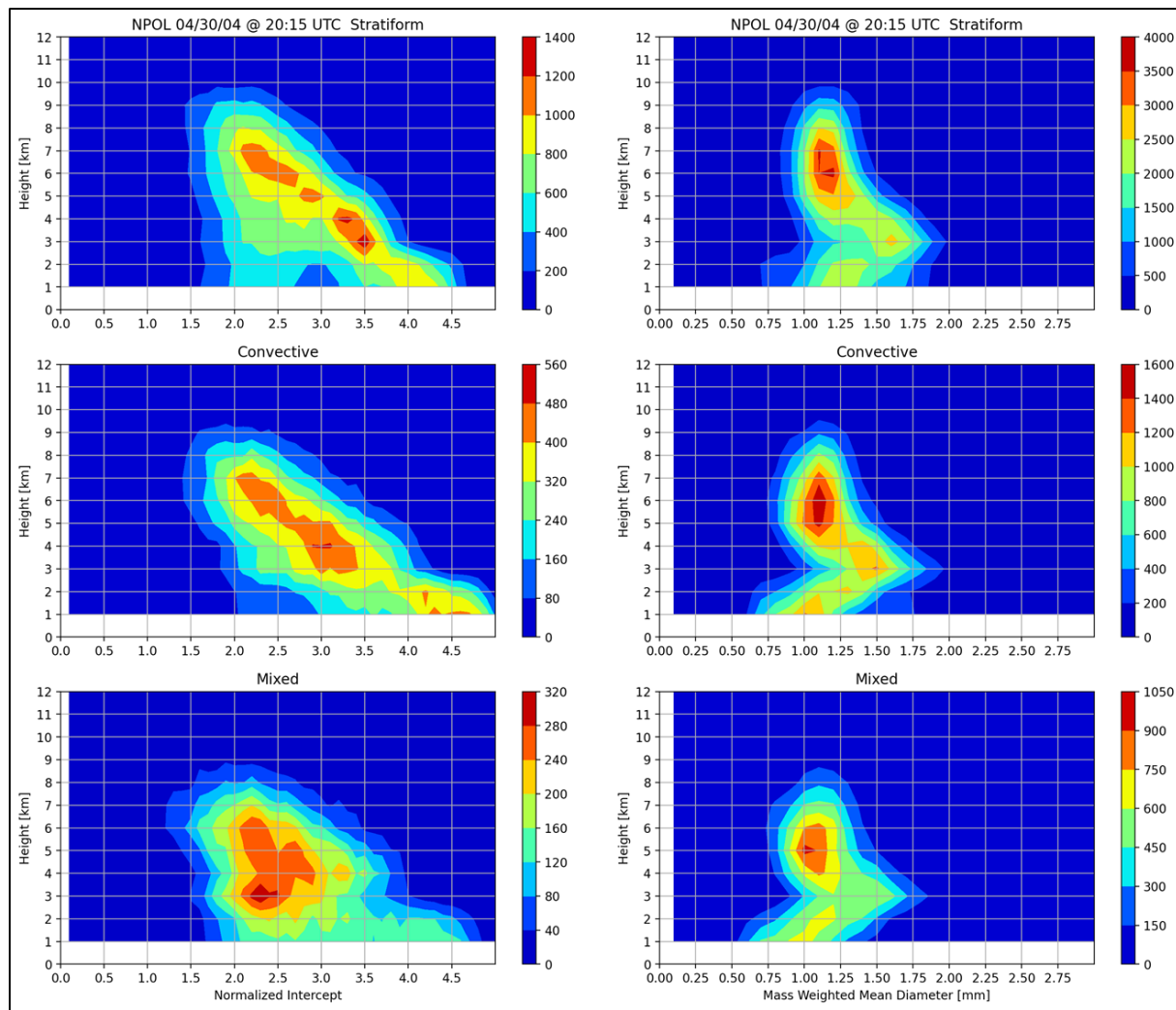
Left panels :  $N_W$  contours

Right panels :  $D_m$  contours

The freezing height on this day was at around 3 km hence the retrieved  $N_W$  and  $D_m$  should be neglected above this height.

*In the rain region below ...*

- i. For both stratiform and convective rain,  $D_m$  decreases from 3 km down to 1 km.
- ii. But for the latter, the rate of decrease (with decreasing height) is noticeably higher, indicating that the break-up is more severe.
- iii. For mixed precipitation, the rate of decrease is more similar to that for convective rain.



# Summary

- ❖ The case study (of line convection embedded within a widespread system) considered here has clearly shown that there is considerable agreement between the texture-based method and the DSD-based method . Only 12% of the gridded radar data pixels showed classification mismatch. When a simple attenuation-correction method (based on differential propagation phase shift) was applied to the S-band data, the percentage of mismatch reduced to 11%.
- ❖ The DSD-based method utilized previously-derived retrievals for the two DSD parameters  $N_W$  and  $D_m$ . Stratiform and convective rain was based on where the  $N_W$ - $D_m$  points lie in relation to the well-established separation line.
- ❖ Though the separation line was determined based on disdrometer data, we have shown that it can also be used for the gridded S-band NPOL radar data.
- ❖ A third category was also introduced to represent the mixed region. They tended to be in areas immediately surrounding the convective rain regions.
- ❖ Contoured Frequency-by-Altitude Diagrams (CFADs) were also generated for the stratiform and convective rain separately. They indicate drop breakup to be a dominant process in the rain region below the freezing height. The rate of decrease (with decreasing height) of  $D_m$  was higher in the case of convective rain, implying that the drop breakup is more severe.

# Summary

- ❖ One caveat in the DSD-based technique is that there are a number of uncertainties which need to be considered when applying this technique. These include (i) variance of 'radar measurement errors'; (ii) retrieval algorithm errors; and (iii) small uncertainties in the assumed separation line.
- ❖ Nevertheless, from this case study, it seems likely that the DSD-based technique can be used for the S-band NPOL gridded data with reasonable accuracy.
- ❖ Further, it can be applied not just to the lowest gridded data but also to higher altitudes, i.e. in the rain region, up to the nominal freezing height.



ECAS  
2021

The 4th International Electronic Conference  
on Atmospheric Sciences  
16-31 JULY 2021 | ONLINE

Chaired by: PROF. DR. ANTHONY R. LUPO

